Appl Biochem Biotechnol (2014) 172:4084–4098
DOI 10.1007/s12010-014-0809-2

Antimicrobial Activity and Physical Characterization of Silver Nanoparticles Green Synthesized Using Nitrate Reductase from *Fusarium oxysporum*

Mohammadhassan Gholami-Shabani · Azim Akbarzadeh · Dariush Norouzian · Abdolhossein Amini · Zeynab Gholami-Shabani · Afshin Imani · Mohsen Chiani · Gholamhossein Riazi · Masoomeh Shams-Ghahfarokhi · Mehdi Razzaghi-Abyaneh

Received: 2 December 2013 / Accepted: 12 February 2014 /
Published online: 9 March 2014

Abstract Nanostructures from natural sources have received major attention due to wide array of biological activities and less toxicity for humans, animals, and the environment. In the present study, silver nanoparticles were successfully synthesized using a fungal nitrate reductase, and their biological activity was assessed against human pathogenic fungi and bacteria. The enzyme was isolated from *Fusarium oxysporum* IRAN 31C after culturing on malt extract-glucose-yeast extract-peptone (MGYP) medium. The enzyme was purified by a combination of ultrafiltration and ion exchange chromatography on DEAE Sephadex and its molecular weight was estimated by gel filtration on Sephacryl S-300. The purified enzyme had a maximum yield of 50.84 % with a final purification of 70 folds. With a molecular weight of 214 KDa, it is composed of three subunits of 125, 60, and 25 KDa. The purified enzyme was successfully used for synthesis of silver nanoparticles in a way dependent upon NADPH using gelatin as a capping agent. The synthesized silver nanoparticles were characterized by

M. Gholami-Shabani · M. Razzaghi-Abyaneh (✉)
Department of Mycology, Pasteur Institute of Iran, Tehran 13164, Iran
e-mail: mrab442@yahoo.com

M. Razzaghi-Abyaneh
e-mail: mrab442@pasteur.ac.ir

M. Gholami-Shabani · A. Akbarzadeh · D. Norouzian · A. Imani · M. Chiani
Department of Nanobiotechnology, Pasteur Institute of Iran, Tehran 13164, Iran

A. Amini
Department of Biotechnology, Pasteur Institute of Iran, Tehran 13164, Iran

Z. Gholami-Shabani
Faculty of Aerospace, Science and Research Campus, Islamic Azad University, Tehran, Iran

G. Riazi
Institute of Biochemistry and Biophysics, University of Tehran, Tehran, Iran

M. Shams-Ghahfarokhi
Department of Mycology, Faculty of Medical Sciences, Tarbiat Modares University, Tehran, Iran

X-ray diffraction, dynamic light scattering spectroscopy, and transmission and scanning electron microscopy. These stable nonaggregating nanoparticles were spherical in shape with an average size of 50 nm and a zeta potential of −34.3. Evaluation of the antimicrobial effects of synthesized nanoparticles by disk diffusion method showed strong growth inhibitory activity against all tested human pathogenic fungi and bacteria as evident from inhibition zones that ranged from 14 to 25 mm. Successful green synthesis of biologically active silver nanoparticles by a nitrate reductase from *F. oxysporum* in the present work not only reduces laborious downstream steps such as purification of nanoparticle from interfering cellular components, but also provides a constant source of safe biologically-active nanomaterials with potential application in agriculture and medicine.

Keywords *Fusarium oxysporum* · Nitrate reductase · Green synthesis · Silver nanoparticles · Antimicrobial activity · Electron microscopy · Fungi · Bacteria

Introduction

The field of nanotechnology is an immensely developing field due to its wide-ranging applications in different areas of science and technology. Nanotechnology is an integration of different fields of science which holds promise in the pharmaceutical industry, medicine, and agriculture [1]. The term nanotechnology is defined as the creation, exploitation, and synthesis of materials at a scale smaller than 1 μm [2]. Nanotechnology has emerged as a division of science and technology to investigate the interactions between nanomaterials and nanobiosystems to explain how nanoparticles of different origin, structure, and chemical properties affect the organization and functions of nanomachinery of cells. Today, a wide spectrum of nanophasic and nanostructure materials is fabricated with the aim to increase nontoxic, safe, and environmentally-friendly bioactive materials [3]. Because of their unique physicochemical properties, nanomaterials have good potential for application in various fields such as optics, electronics, mechanics, and catalysis medicine [1].

Different types of nanomaterials including copper, zinc, titanium, magnesium, gold, and silver have been applied in biological systems [4]. These materials exhibited antimicrobial activity against a wide array of pathogenic microorganisms such as fungi, bacteria, and viruses [5]. Today, silver nanoparticles are commercially used as antimicrobial agents in most of the public places such as elevators and railway stations in the world. They are used as antimicrobial agents in surgically implanted catheters in order to reduce the infections caused during surgery and are proposed to possess antifungal, anti-inflammatory, anti-angiogenic, and anticancer effects as well as anti-permeability activity against gases essential for microbial growth such as oxygen [6, 7].

In recent years, interest in employment of biological systems including microorganisms as cell factories in production of nanoparticles with new biological activities has increased dramatically [8]. Microorganisms (bacteria and fungi) and plants are in the first line of investigation for synthesis of green nanoparticles via both extracellular and intracellular routes [9–16]. The process of synthesis is less labor-intensive, low-cost technique, nontoxic, and is more of a greener approach making the biological method superior compared with the physical and chemical methods of synthesis. Different types of biogenic nanomaterials including cadmium sulfide, copper, zinc, titanium, magnesium, gold, platinum, and silver have been applied in biological systems [4]. Silver nanoparticles are the most important types of nanomaterials produced by microorganisms because they are active against most of the

nosocomial infections related to catheters. They predominantly accumulate at the site of insertion, so are protective against infection with no risk of systemic toxicity [17]. Unfortunately, microbial synthesis of silver nanoparticles is restricted to a small portion of biodiversity due to the absence of mechanisms of silver resistance against silver ions in the majority of microorganisms. Likewise, reduction of silver ions by biomolecules of microorganisms such as enzymes, proteins, amino acids, polysaccharides, and vitamins occurs via complex pathways involving electron transfer mainly as a consequence of conversion of NADPH/NADH to $NADP^+/NAD^+$ [18–20].

Employment of microbial enzymes for synthesis of silver nanoparticles is a new field with growing importance. The enzymatically-produced nanoparticles are useful for heterogeneous (immobilized enzymes) and homogeneous (soluble-free enzymes) catalysis with application in industrial chemical processes and chemical reactions in human body by serving as site of catalysis or as a support for catalytic processes, and they are suitable for nonlinear optics as well [21]. The biological agents including fungi and bacteria secrete a large number of enzymes, which are involved in enzymatic reduction of metals ions as an essential step for efficient production of silver nanoparticles [5]. A widely accepted mechanism for the synthesis of silver nanoparticles is the role of an interesting enzyme named nitrate reductase, which catalyzes the conversion of nitrate to nitrite in the nitrogen cycle by the relevant enzymes of microorganisms [22–24]. Nitrate reductase is a multidomain enzyme comprising the prosthetic groups molybdopterin, Fe-heme, and FAD (flavin adenine dinucleotide) in a 1:1:1 stoichiometry that mediates an electron transfer from NAD(P)H to nitrate [25].

In the case of fungi, nitrate reductase is found to be responsible for the extracellular synthesis of nanoparticles through bioreduction of metal ions [22, 23, 26–28]. Although the enzyme in the form of culture supernatant is used to produce silver nanoparticles in fungi and some bacteria such as *Bacillus licheniformis* [21, 23], very little has been documented about its application for green synthesis of bioactive nanoparticles in purified form.

In the present study, a nitrate reductase purified from *Fusarium oxysporum* was successfully used for synthesis of biologically active silver nanoparticles that showed strong inhibitory activity toward pathogenic fungi and bacteria in a NADPH-dependent manner using gelatin as a capping agent. The synthesized silver nanoparticles were characterized by X-ray diffraction, dynamic light scattering spectroscopy, and transmission and scanning electron microscopy.

Materials and Methods

Fungal Strain and Culture Conditions

F. oxysporum IRAN31C was obtained from the Microbial Culture Collection of the Iranian Research Institute of Plant Protection (IRIPP), Tehran, Iran. The fungus was initially grown on Sabouraud dextrose agar for 5 days at 28 °C. The mycelia were separated from culture medium and aseptically transferred to a liquid medium containing (per liter) yeast extract 3 g, malt extract 3 g, peptone 5 g, and glucose 10 g. The submerged cultures were incubated for 4 days at 26 °C with shaking (200 rpm) [29]. Fungal biomass was washed thrice with sterile distilled water and subcultured to new cultures at the above conditions for 2 days. Finally, cultures were centrifuged (4,000 rpm, 60 min, 4 °C). Culture filtrate and fungal mycelia were assessed for the presence of nitrate reductase.

Purification of Nitrate Reductase

Enzyme Extraction from Fungal Mycelia and Culture Media

Fungal mycelia were powdered by mortar and pestle in the presence of liquid nitrogen. One gram of powdered mycelia was added to 10 ml of Tris-HCl buffer (50 mM, pH 8.8) and kept on shaker for 15 min. A mixture of EDTA (5 mM), lysozyme (Sigma-Aldrich, 0.5 mg/ml), and DNase + RNase solution (50 μg/ml) was added to the mycelia suspension and stirred slowly for 30 min to achieve cell destruction. The derbies were separated by centrifugation (3,000 rpm, 10 min). The supernatant (cytoplasmic extract) was suspended in phosphate buffer (50 mM, pH 7.2) containing 0.1 mM 2-mercaptoethanol and 0.1 mM phenylmethylsulfonyl fluoride (PMSF). Triton X-100 was added to the mixture at a final concentration of 2 %. The mixture was stirred at 100 rpm for 30 min and then centrifuged (25,000 rpm, 2 h at 4 °C). The obtained supernatant (130 ml) was added to the culture filtrate (350 ml), concentrated in the retentate by ultrafiltration (cutoff 100,000 Da) and used for purification of nitrate reductase. The amount of protein was estimated by Lowry's method using bovine serum albumin as standard.

Ion Exchange Chromatography

Ion exchange chromatography was used to purify nitrate reductase from *F. oxysporum* IRAN31C. The column (10×2.5 cm) was packed with DEAE Sephadex A-50 preequilibrated with phosphate buffer (50 mM, pH 7.2). The enzyme source (concentrated fungal extract from previous step) was loaded onto the column, washed with phosphate buffer, and eluted with the gradient of NaCl (0→2 M) prepared in the same buffer at a flow rate of 1 ml/min. Fractions of 2 ml were collected and their protein contents (OD at 280 nm), enzyme activity, conductivity, and pH determined. The active fractions were pooled, dialyzed against phosphate buffer, and finally concentrated using Amicon Ultra-15 centrifugal filter units (Millipore).

Assessment of Nitrate Reductase Activity

The activity of nitrate reductase was determined colorimetrically through the reduction of nitrate to nitrite by methyl viologen as an electron donor [30]. Nitrite was finally assessed as the final product of enzyme activity. All reaction mixtures were prepared in deionized water unless otherwise specified. The reaction mixture contained 0.5 ml of 50 mM phosphate buffer pH 7.2, 0.5 ml of 50 mM sodium nitrate solution ($NaNO_3$) as enzyme substrate, 0.2 ml of 0.05 % (*w*/*v*) methyl viologen solution (Sigma-Aldrich) as electron donor, 10 μl of 0.8 % (*w*/*v*) Cleland's reagent (dithiothreitol, Calbiochem) as reducing agent, and 1.1 ml fungal extract as the source of enzyme. The reaction was started by the addition of 0.1 ml reagent consisting of 0.8 % (*w*/*v*) sodium bicarbonate and 0.8 % (*w*/*v*) sodium dithionate which was swirled slowly till blue color appeared. After incubation at 37 °C for 60 min, the reaction was stopped by mixing the reaction mixture vigorously until blue color disappeared completely. Two milliliter sulfonic acid (1.0 % *w*/*v* in 20 % HCl, *v*/*v* in deionized water) as detergent, 2 ml *N*-naphthyl ethylenediamine (Sigma-Aldrich) as diazonium coupling reactive agent, and 0.129 % HCl were added to the reaction mixture, and the adsorption was read at 540 nm after 10 min. One unit of nitrate reductase activity was defined as the amount of enzyme reduces 1 μmol of nitrate to nitrite per minute under assay condition.

Molecular Weight Determination

The purity and apparent molecular weight of nitrate reductase was checked by SDS-PAGE according to Laemmli using protein marker as standard [31]. The molecular weight of purified nitrate reductase was determined by size exclusion chromatography on Sephacryl S-300 which was equilibrated with 50 mM sodium phosphate buffer (pH 7.2) containing 0.1 mM 2-mercaptoethanol and 0.1 mM PMSF. Purified nitrate reductase (1 mg/ml) was loaded onto Sephacryl S-300 column (2×100 cm) and eluted with phosphate buffer at the rate of 0.25 ml/min. Fractions of 0.5 ml were collected. Standard globular proteins of known molecular weights were used to calibrate the column.

Synthesis and Characterization of Silver Nanoparticles

For synthesis of the silver nanoparticles, reaction mixture (3 ml) containing 0.2 M phosphate buffer (pH 7.2), 1 mM silver nitrate as the enzyme substrate, 100 μg gelatin as a capping agent, 1 mM 4-hydroxyquinoline as an electron carrier, 1 mM NADPH as enzyme cofactor, and 100 μg of purified fungal nitrate reductase was incubated at 25 °C for 5 h. The reaction was also carried out in the absence of each of the individual components viz. nitrate reductase, NADPH, 4-hydroxtquinoline, and gelatin. A blank containing heat-treated denatured enzyme was also included in the experiment. After completing the reaction, synthesized nanoparticles were collected by centrifugation at 8,000 rpm for 30 min and washed twice with sterile distilled water. Proteins were removed by treating with 80 % (*v*/*v*) ethanol. Synthesis of silver nanoparticles was confirmed by calculating the absorption at 415 nm. The synthesized silver nanoparticles were characterized by dynamic light scattering spectroscopy (Zetasizer), X-ray diffraction, and scanning and transmission electron microscopy. By using the X-ray diffraction, the mean size of nanoparticles was calculated by Scherer formula ($D = \frac{0.9\lambda}{\beta\cos\theta}$) where λ is the wavelength of X-ray, θ is the diffraction angle, $\beta = \sqrt{Bm^2 + Bs^2}$ is the corrected halfwidth of the observed halfwidth, Bm is that of the (111) reflection in samples, and Bs is that of the (111) reflection in a standard.

Antimicrobial Activity of Silver Nanoparticles

Antifungal Activity

The antifungal activity of silver nanoparticles was evaluated against the following human pathogenic strains: *Aspergillus fumigatus* PTCC 5009, *Alternaria alternata* PTCC 5224, *Trichoderma parceramosum* PTCC 5140, *Penicillium citrinum* PTCC 5304, *Paecilomyces variotii* PTCC 5126, *Candida albicans* PTCC 5027, *Candida glabrata* PTCC 5297, *Trichophyton mentagrophytes* PTCC 5054, and *Microsporum gypseum* PTCC 5070. These fungal strains were obtained from Persian Type Culture Collection (PTCC), Iran. Cultures were maintained on Potato dextrose agar (PDA) slants and they were subcultured before use. Antifungal activities of synthesized silver nanoparticles were assessed by disk diffusion method using blank disks (6.0 mm Dia., HiMedia, India) on Mueller Hinton agar (MHA) supplemented with 2 % glucose and 0.5 μg/ml methylene blue. Addition of methylene blue made the zones of inhibition clearer and easier to measure precisely. Disks of known antifungals (10 μg/disk; 6.0 mm Dia., MAST Diagnostics) were used as positive controls. Agar plates were swab-inoculated with a suspension of fungal conidia of filamentous fungi (10^5 conidia/ml) or yeast cells (for *Candida* sp. adjusted to the turbidity of a 0.5 McFarland

standard). The plates were allowed to dry before placing the antifungal disks. Sterile blank disks impregnated in silver nanoparticle solution (50 μg/disk) and standard antifungal disks were placed on the surface of agar plates separately. The plates were incubated for 48–96 h at 30 to 35 °C. The interpretive criteria were based on the diameter of zone of inhibition of growth around the disks.

Antibacterial Activity

The antibacterial activity of silver nanoparticles was evaluated against the following human pathogenic strains: *Escherichia coli* PTCC 1330, *Pseudomonas aeruginosa* PTCC 1310, *Staphylococcus aureus* PTCC 1431, *Salmonella typhi* PTCC 1735, and *Klebsiella pneumoniae* PTCC 1290. These bacteria were obtained from the Persian Type Culture Collection (PTCC), Iran. Cultures were maintained on LB agar slants and they were subcultured before use. Agar plates were swab-inoculated with a suspension of bacterial cells adjusted to the turbidity of a 0.5 McFarland standard. Blank disks (6.0 mm Dia., HiMedia) impregnated in silver nanoparticle solution (2.5 mg/ml) were placed on the agar surface and incubated for 24 h at 35 °C. Standard disks of antibacterial containing 20 μg of each amoxicillin, streptomycin, and ofloxacin were used as positive controls. After incubation at 37 °C for 24 h, the different levels of zone of inhibition of growth around disks were measured as an index of antibacterial activity.

Results

Purification of Nitrate Reductase from *F. oxysporum*

In the present study, a nitrate reductase with molecular weight of 214 KDa was purified from *F. oxysporum* and successfully used for synthesis of functional silver nanoparticles. The steps involved in purifying the fungal enzyme are summarized in Table 1. Fungal extract used for the enzyme purification was a mixture of fungal culture filtrate (350 ml; enzyme activity of 312 U/ml/min) and the mycelia extract (130 ml; enzyme activity of 872 U/ml/min). After fractionation by ion exchange chromatography on DEAE Sephadex A-50, fractions containing nitrate reductase activity were collected at NaCl gradient concentrations of 1.15–1.35 M. The maximum enzyme activity was obtained in fractions that eluted at 1.25 M NaCl (Fig. 1). The purified enzyme had a maximum yield of 50.84 % with a final purification fold of 70. For molecular weight determination, fractions containing more than 20 % enzyme activity were

Table 1 Purification steps of nitrate reductase from *Fusarium oxysporum* IRAN 31C cultured on MGYP medium

Fraction	Total volume (ml)	Total protein (mg)	Activity (U/ml/min)	Specific activity (units/mg protein)	Yield (%)	Purification (fold)
Fungal extract[a]	480	467	1184	2.53	100	1.0
Ultrafiltration	10	32	722	22.56	60.97	8.91
DEAE Sephadex A-50 chromatography	2.0	3.4	602	177.10	50.84	70.0

[a] Fungal extract used for enzyme purification was a mixture of fungal culture filtrate (350 ml; enzyme activity of 312 U/ml/min) and the extract from fungal mycelia (130 ml; enzyme activity of 872 U/ml/min)

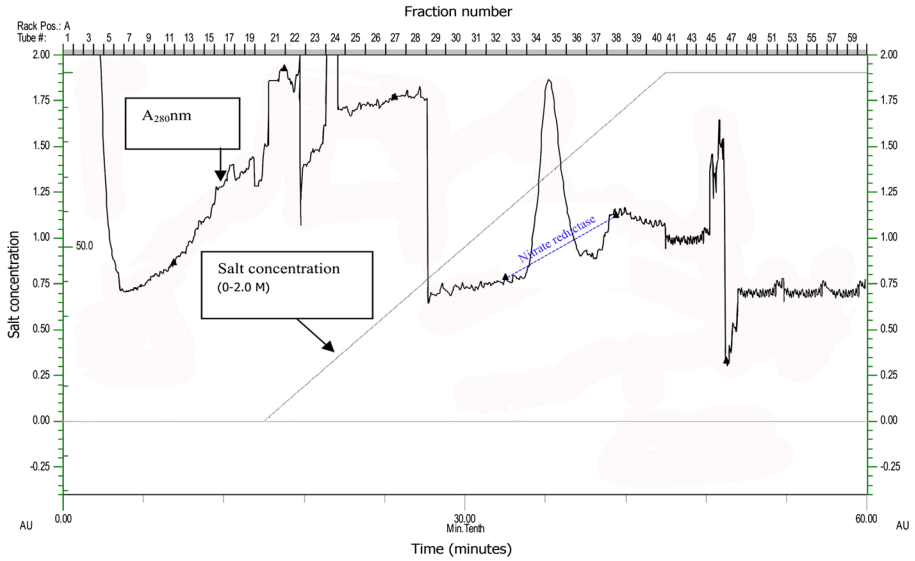

Fig. 1 Elution profile of nitrate reductase from DEAE Sephadex A-50. Data of fraction numbers, elution time, and salt concentration are shown in details. Linear gradient elution of enzyme by salt concentrations from 0 to 2.0 M is also indicated

pooled and loaded on Sephacryl S-300 column. The molecular weight of purified enzyme was estimated to be 214 KDa. As shown in Fig. 2, SDS-PAGE analysis revealed the presence of three subunits with the molecular weights of 125, 60, and 25 KDa. The 125 KDa disappeared after heat treatment as shown in lane 6. It may be precipitated in the pellet as a consequence of heat denaturation. Purified nitrate reductase was stable over the temperature range of 20 to 60 °C maintaining 50 % of its original activity. The optimum temperature for the enzyme activity was found to be 45 °C (Fig. 3a). The enzyme was stable in phosphate buffer (50 mM, pH 7.2) and maintained 50 % of its original activity at pH range of 5 to 9 indicating the suitable

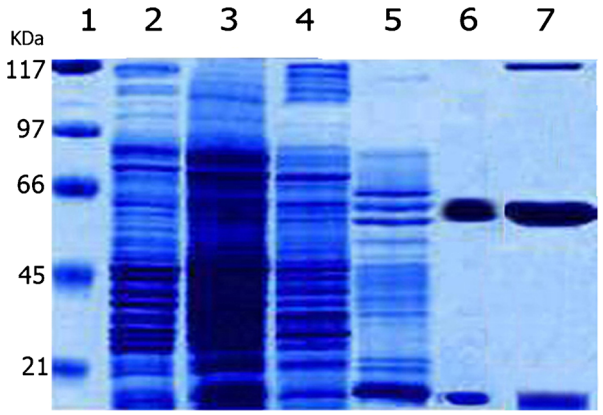

Fig. 2 SDS-PAGE pattern of proteins during purification steps of nitrate reductase from *F. oxysporum*. *Lane 1* shows the standard protein molecular weight markers (BioRad, USA). *Lanes 2* to *6* show culture filtrate, fungal mycelia homogenate, ultrafiltered extract, heat-treated extract, and heat-treated extract after ion exchange chromatography. *Lane 7* shows purified enzyme after ion exchange chromatography on DEAE Sephadex A-50 which is composed of three subunits of 125, 60, and 25 KDa

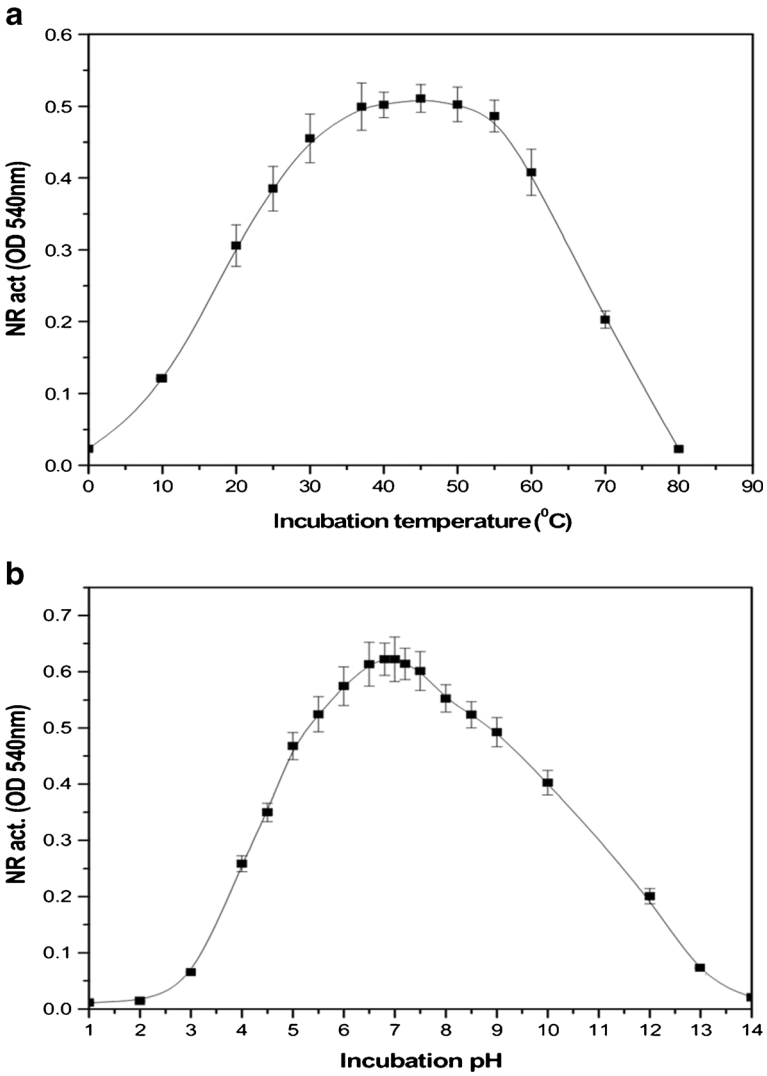

Fig. 3 Effects of temperature (**a**) and pH (**b**) on nitrate reductase activity purified from *F. oxysporum*

stability of enzyme over different pH levels (Fig. 3b). These results show the high compatibility and thermal stability of nitrate reductase of *F. oxysporum* IRAN 31C.

Synthesis and Characterization of Silver Nanoparticles by Nitrate Reductase

Proposed mechanism of nitrate reductase based formation of silver nanoparticles has been demonstrated in Fig. 4. Formation of silver nanoparticles in the presence of purified fungal nitrate reductase was spectrophotometrically followed (Fig. 5). The reaction mixture was colorless before adding of ionic silver. It turned to brownish-yellow after formation of silver nanoparticles as a consequence of surface plasmon resonance of metallic nanoparticles. As shown in Fig. 5, the maximum absorbance of

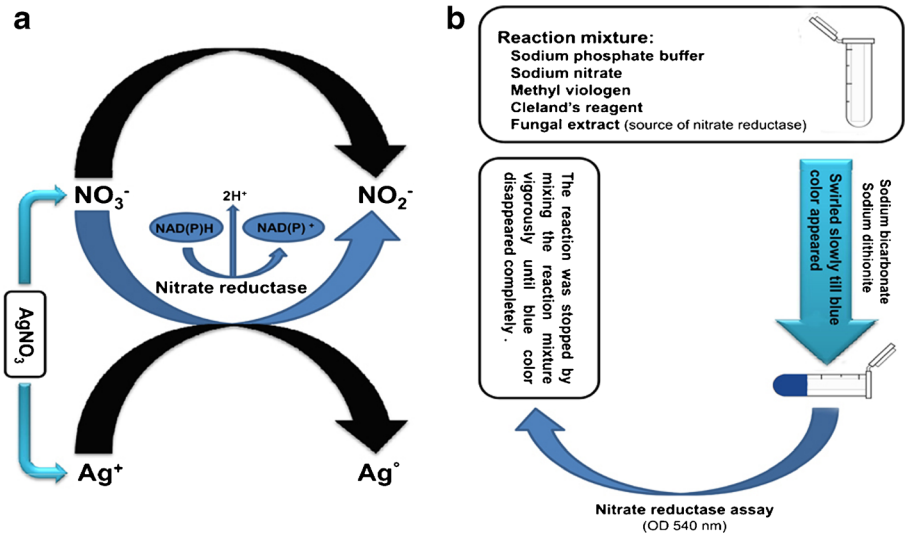

Fig. 4 Proposed scheme of nitrate reductase-mediated formation of silver nanoparticles is demonstrated in (**a**). Colorimetric measurement of nitrate reductase activity in *F. oxysporum* is shown in (**b**)

surface plasmon resonance was in the wavelength of 415 nm and after 5 h, the reaction was stabilized. Silver nanoparticle solution was stable, and over 1 month, no precipitate was observed. The absence of surface plasmon resonance at 415 nm in the reaction mixture devoid of nitrate reductase clearly shows that reduction of silver is coupled to the reduction of nitrate to nitrite. The lack of surface plasmon resonance at

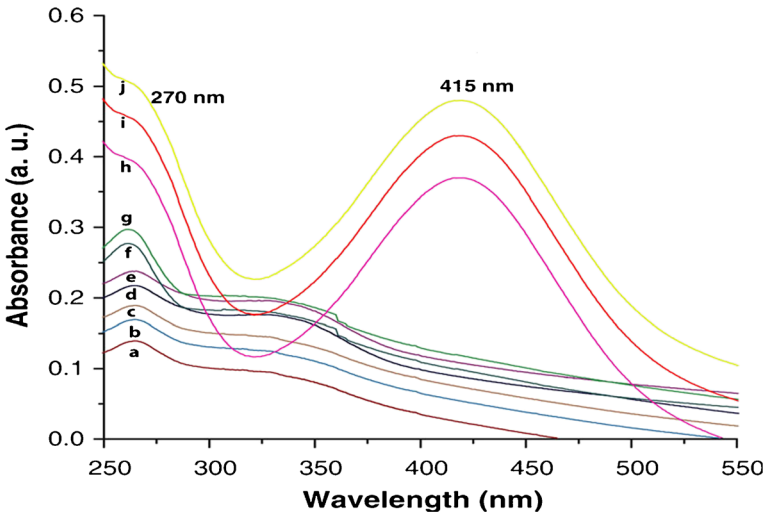

Fig. 5 UV-visible spectrum data of silver nanoparticle formation by purified nitrate reductase from *F. oxysporum*: Conversion of silver nitrate to NO_2 ions and silver nanoparticles by purified nitrate reductase after 1 h (*f*), 2 h (*g*), 3 h (*h*), 4 h (*i*), and 5 h (*j*). Controls without purified enzyme (*a*), NADPH (*b*), gelatin (*c*), 4-hydroxyquinoline (*d*), and denatured enzyme (*e*) show no enzymatic activity in the absence of all reaction mixtures

415 nm in the reaction mixtures in the absence of NADPH, 4-hydroxyquinoline, or gelatin showed that reduction of NADPH to $NADP^+$ is necessary for the process of silver nanoparticle formation. 4-hydroxyquinoline probably act as an electron transfer agent which means that it may transfer electrons produced during reduction of nitrate to Ag^+ ions to form Ag^o. Produced silver nanoparticles were capped at nanoscale by gelatin to avoid unwanted aggregation. Gelatin is not directly involved in nanoparticle formation, but it is completely necessary to avoid the formation of insoluble nanoparticles which lacks any absorbance at 415 nm as they precipitated in the mixture.

Transmission (TEM) and scanning (SEM) electron micrographs of silver nanoparticles showed mainly single silver nanoparticles and less frequently some silver aggregates. The SEM (Fig. 6a) showed high-density silver nanoparticles synthesized by the nitrate reductase which further confirms the efficient development of silver nanostructures. The TEM micrographs showed that silver nanoparticles were spherical in shape and they had appropriate scattering without any obvious aggregation (Fig. 6b). The approximate size of silver nanoparticles was estimated by 50 nm in TEM.

According to the dynamic light scattering results, the nanoparticles had an average size of 50 nm with zeta potential of −34.3±0.2 (Fig. 7a). The presence of silver nanoparticles was further confirmed by XRD spectrum as compared to the standard XRD spectrum (Fig. 7b). Scattering XRD spectrum of the sample showed four peaks at Bragg's angles which conformed to metallic silver phase (JCPDS file no. 04-0783). They were related to crystalline planes (111), (200), (220), and (311), and the intensity of peaks for plane (111) was stronger. Peaks arising from 2θ at 38, 34, 64, and 77 were crystalline planes of (111), (200), (220), and (311), respectively. These peaks caused by Bragg scattering indicate the formation of crystalline silver nanoparticles with spiral structure and an A equal to 4.086. No phases of silver oxide and any other compound between silver and Tin were observed. The results showed that mean particles size was around 50 nm.

Antimicrobial Activity of Synthesized Silver Nanoparticles

As indicated in Table 2, silver nanoparticles showed strong antifungal activity against human pathogenic fungi. The range of inhibition zones were observed as 17–25 mm.

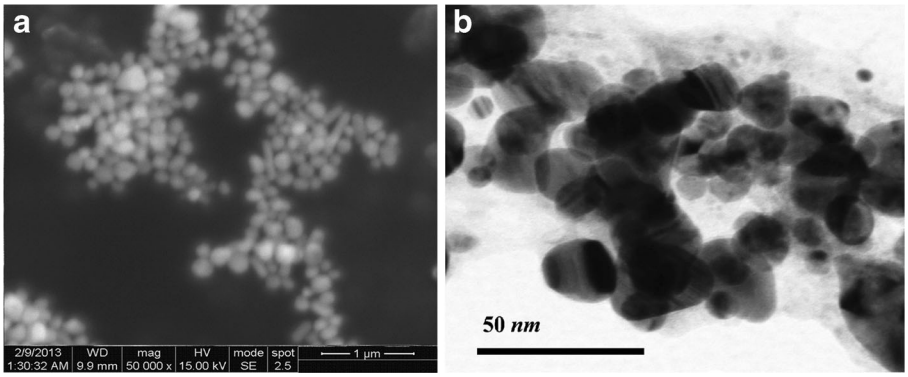

Fig. 6 Scanning (**a**) and transmission (**b**) electron micrographs characterize silver nanoparticles synthesized by nitrate reductase of *F. oxysporum*

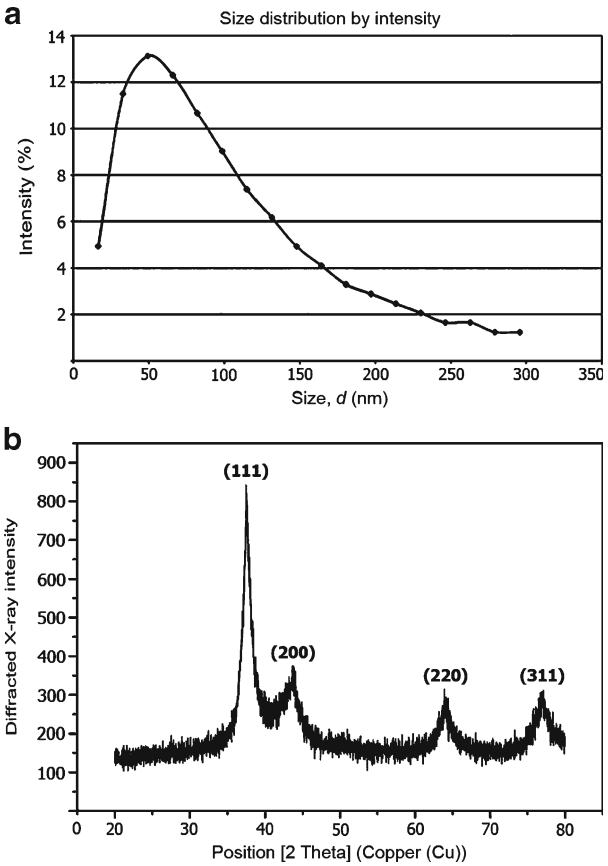

Fig. 7 Dynamic light scattering spectrum of silver nanoparticles synthesized by purified nitrate reductase of *F. oxysporum* showing maximum scattering at 50 nm (**a**). X-ray diffraction spectrum of silver nanoparticles synthesized by purified nitrate reductase of *F. oxysporum* which indicates a good correlation with the patterns of silver nanoparticles from other sources (**b**)

The minimum inhibition zone of 17 mm was observed for *M. gypseum*, while two fungi, i.e., *T. mentagrophytes* and *P. variotii* showed the maximum inhibition of 25 mm. Interestingly, synthesized nanoparticles inhibited the growth of nearly all fungi more strongly than that of known tested antifungal drugs including azoles and amphotericin B. Table 3 shows antibacterial activity of the nanoparticles against pathogenic bacteria. A clear zone of inhibition ranged from 14 to 23 mm was observed for tested bacteria. *S. typhi* showed the least inhibition zone of 14 mm; whereas *S. aureus* had the highest inhibition zone of 23 mm. A comparable effect with known antibacterials was observed in the present study. Silver nitrate solution showed lower antimicrobial activity against tested fungi and bacteria in comparison with the synthesized silver nanoparticles (Tables 2 and 3).

Discussion

In the present study, we achieved the green synthesis of silver nanoparticles using nitrate reductase purified from a hyaline Hyphomycete, *F. oxysporum*. These nanoparticles showed strong antimicrobial activity against a wide array of human pathogenic fungi and bacteria.

Table 2 Antifungal activity of silver nanoparticles synthesized by nitrate reductase purified from *Fusarium oxysporum* against some selected fungal pathogens[a]

Fungus		Zones of inhibition (mm)				
	Ag nanoparticles[b]	$AgNO_3$ solution[c]	Itraconazole[d]	Fluconazole[d]	Ketoconazole[d]	Amphotericin B[d]
A. alternata	22	6	10	0	15	10
A. fumigatus	24	8	30	14	30	10
P. citrinum	24	7	13	0	25	7
P. variotii	25	8	11	0	9	13
T. parceramosum	18	6	4	0	8	8
C. albicans	22	6	9	14	17	7
C. glabrata	20	7	9	18	20	10
T. mentagrophytes	25	7	14	30	20	20
M. gypseum	17	6	13	18	14	11

[a] Disk diffusion method

[b] Blank disks impregnated with Ag nanoparticle solution (50 μg/disk) were used

[c] Blank disks impregnated with $AgNO_3$ solution (50 μg/disk) were used

[d] Standard disks (10 μg/disk, HIMEDIA India) of known antifungals were used as control

Although the synthesis of nanoparticles using the biological methods is environmentally friendly compared with the routine physicochemical methods, there are certain key areas of research which need to be pointed out. Nowadays, the majority of nanoparticles are produced by using fungal and bacterial cells but not purified enzymes. This may cause several problems especially when the process needs to be scaled up for industrial applications. The major problem in cell-based procedures is binding of the synthesized nanoparticles to the microbial biomass. This means that further steps of breaking down the microbial cells and subsequent isolation of nanoparticles is necessary for purification of nanoparticles.

Table 3 Antibacterial activity of silver nanoparticles synthesized by nitrate reductase purified from *Fusarium oxysporum* against some selected bacterial pathogens[a]

Bacteria		Zones of inhibition (mm)			
	Ag nanoparticles[b]	$AgNO_3$ solution[c]	Ofloxacin[d]	Amoxicillin[d]	Streptomycin[d]
Staphylococcus aureus	23	7	14	5	12
Escherichia coli	19	8	13	14	16
Pseudomonas aeruginosa	16	6	13	6	16
Klebsiella pneumoniae	17	5	14	15	10
Salmonella typhi	14	6	15	14	12

[a] Disk diffusion method

[b] Blank disks impregnated with Ag nanoparticle solution (50 μg/disk) were used

[c] Blank disks impregnated with $AgNO_3$ solution (50 μg/disk) were used

[d] Standard disks (20 μg/disk, HIMEDIA India) of known antibacterials were used as control

Furthermore, Ag ions have limitations for applying in the biological systems because they are toxic for the biomass at concentrations more than 1 mM [21]. For overcoming these problems, microbial culture supernatants have been successfully used for nanoparticle synthesis by several researchers. Although culture supernatants are superior to microbial biomass in nanoparticle synthesis due to the lower costs and simplicity for application and maintenance, they suffer from large limitations including the limited numbers of microorganisms possessing essential secretory proteins for nanoparticle synthesis as well as necessity for downstream processes for purification and cleansing the final product. In contrast to purified enzymes, both microbial biomass and culture supernatant cannot be reused which makes the process of nanoparticle synthesis noneconomic especially in industrial application [32].

Our enzymatically synthesized nanoparticles have several advantages over those routinely produced by microbial biomasses and culture supernatants. Besides considerable decrease of the downstream steps needed for purification of produced nanoparticles, they have high potential for industrial applications as the nitrate reductase can be immobilized for recycling in nanoparticle synthesis. Likewise, our cell-free synthesized nanoparticles were spherical in shape with an average size of 50 nm which provides a wide surface for their adhering, penetrating, and killing hazardous microorganisms as shown against pathogenic fungi and bacteria in the present work. Silver nanoparticles showed comparable results with known antifungal and antibacterial drugs, indicating their potency as good alternatives for application as antimicrobial agents.

Large-scale synthesis of biogenic nanoparticles from microorganisms has been a great challenge for several years. To our knowledge, limited data have been reported on green synthesis of silver nanoparticles at industrial scale. In a report from Huang, leaves extract of cinnamon have been successfully used in small reactors for biosynthesis of silver nanoparticles [33]. In the present study, purified fungal nitrate reductase had an optimum temperature of 45 °C, while the optimum temperature of this enzyme from *E. coli* is reported to be 23 °C [34]. With respect to no limitation for reuse of our purified fungal nitrate reductase in nanoparticle synthesis and its thermostability and wide pH range of activity, it is very well suited for nanoparticle synthesis in industrial scale in immobilized form.

Taken together, successful green synthesis of biologically active silver nanoparticles by a nitrate reductase from *F. oxysporum* in the present work not only reduces downstream steps for purification of the nanoparticles from the other proteins, but also provides a constant source of safe biologically active nanomaterials for large-scale production with potential application in agriculture and medicine.

Acknowledgments This work was supported financially by the Pasteur Institute of Iran (Grants Nos. 586 and 647).

References

1. Mohanpuria, P., Rana, N. K., & Yada, S. K. (2008). Biosynthesis of nanoparticles: technological concepts and future applications. *Journal of Nanoparticle Research, 10*, 507–517.
2. Rai, M., Yadav, A., & Gade, A. (2008). Current trends in phytosynthesis of metal nanoparticles. *Critical Reviews in Biotechnology, 28*, 277–284.
3. Sinha, S. H., Pan, L., Chanda, P., & Sen, S. K. (2009). Nanoparticles fabrication using ambient biological resources. *Journal of Applied Biosciences, 19*, 1113–1130.
4. Silver, S., Phung, L. T., & Silver, G. (2006). Silver as biocides in burn and wound dressings and bacterial resistance to silver compounds. *Journal of Industrial Microbiology & Biotechnology, 33*, 627–634.

5. Rai, M., Yadav, A., & Gade, A. (2009). Silver nanoparticles as a new generation of antimicrobials. *Biotechnology Advances, 27*, 76–83.
6. Kalishwaralal, K., Banumathi, E., Pandian, S. B. R. K., Deepak, V., Muniyandi, J., & Eom, S. H. (2009). Silver nanoparticles inhibit VEGF induced cell proliferation and migration in bovine retinal endothelial cells. *Colloids and Surfaces, B: Biointerfaces, 73*, 51–57.
7. Sheikpranbabu, S., Kalishwaralal, K., Venkataraman, D., Eom, S. H., Park, J., & Gurunathan, S. (2009). Silver nanoparticles inhibit VEGF-and IL-1b-induced vascular permeability via Src-dependent pathway in porcine retinal endothelial cells. *Journal of Nanobiotechnology, 7*, 8.
8. Vaidyanathan, R., Kalishwaralal, K., Gopalram, S. H., & Gurunathan, S. (2009). Nanosilver—the burgeoning therapeutic molecule and its green synthesis. *Biotechnology Advances, 27*, 924–937.
9. Mukherjee, P., Ahmad, A., Mandal, D., Senapati, S., Sainkar, S. R., Khan, M. I., et al. (2001). Bioreduction of $AuCl_4^-$ ions by the fungus *Verticillium* sp. and surface trapping of the gold nanoparticles formed. *Angewandte Chemie International Edition, 40*, 3585–3588.
10. Chen, J. C., Lin, Z. H., & Ma, X. X. (2003). Evidence of the production of silver nanoparticles via pretreatment of *Phoma* sp. 32883 with silver nitrate. *Letters in Applied Microbiology, 37*, 105–108.
11. Mouxing, F., Qingbiao, L., Daohua, S., Yinghua, L., Ning, H., Xu, D., et al. (2006). Rapid preparation process of silver nanoparticles by bioreduction and their characterizations. *Chinese Journal Chemical Engineering, 14*, 114–117.
12. Birla, S., Tiwari, V. V., Gade, A. K., Ingle, A. P., Yadav, A. P., & Rai, M. K. (2009). Fabrication of silver nanoparticles by *Phoma glomerata* and its combined effect against *Escherichia coli*, *Pseudomonas aeruginosa* and *Staphylococcus aureus. Letters in Applied Microbiology, 48*, 173–182.
13. Jha, A. K., Prasad, K., Prasad, K., & Kulkarni, A. R. (2009). Plant system: nature's nanofactory. *Colloids and Surfaces, B: Biointerfaces, 73*, 219–223.
14. Shaligram, N. S., Bule, M., Bhambure, R. M., Singhal, R. S., Singh, S. K., Szakacs, G., et al. (2009). Biosynthesis of silver nanoparticles using aqueous extract from the compactin producing fungal strain. *Process Biochemistry, 44*, 939–948.
15. Ogi, T., Saitoh, N., Nomura, T., & Konishi, Y. (2010). Room-temperature synthesis of gold nanoparticles and nanoplates using *Shewanella* algae cell extract. *Journal of Nanoparticles Research, 12*, 2531–2539.
16. Pandian, S. R. K., Deepak, V., Kalishwaralal, K., Viswanathan, P., & Gurunathan, S. (2010). Mechanism of bactericidal activity of silver nitrate—a concentration dependent bi-functional molecule. *Brazilian Journal of Microbiology, 41*, 805–809.
17. Roe, D., Karandikar, B., Bonn-Savage, N., Gibbins, B., & Roullet, J. B. (2008). Antimicrobial surface functionalization of plastic catheters by silver nanoparticles. *Journal of Antimicrobial Chemotherapy, 61*, 869–876.
18. Matsumura, Y., Yoshikata, K., Kunisak, S., & Tsuchido, T. (2003). Mode of bactericidal action of silver zeolite and its comparison with that of silver nitrate. *Applied and Environmental Microbiology, 69*, 4278–4281.
19. Fayaz, M., Tiwary, C. S., Kalaichelvan, P. T., & Venkatesan, R. (2010). Blue orange light emission from biogenic synthesized silver nanoparticles using *Trichoderma viride. Colloids and Surfaces, B: Biointerfaces, 75*, 175–178.
20. Thakkar, K. N., Mhatre, S. S., & Parikh, R. Y. (2010). Biological synthesis of metallic nanoparticles. *Nanomedicine, 6*, 257–262.
21. Kalimuthu, K., Babu, R. S., Venkataraman, D., Bilal, M., & Gurunathan, S. (2008). Biosynthesis of silver nanocrystals by *Bacillus licheniformis. Colloids and Surfaces, B: Biointerfaces, 65*, 150–153.
22. Duran, N., Marcato, P. D., Alves, O. L., DeSouza, G., & Esposito, E. (2005). Mechanistic aspects of biosynthesis of silver nanoparticles by several *Fusarium oxysporum* strains. *Journal of Nanobiotechnology, 3*, 1–8.
23. Kumar, A. S., Abyaneh, M. K., GosaviSulabha, S. W., Ahmad, A., & Khan, M. I. (2007). Nitrate reductase mediated synthesis of silver nanoparticles from $AgNO_3$. *Biotechnology Letters, 29*, 439–445.
24. Moteshafi, H., Mousavi, S. M., & Shojaosadati, S. A. (2012). The possible mechanisms involved in nanoparticles biosynthesis. *Journal of Industrial and Engineering Chemistry, 18*, 2046–2050.
25. Cannons, A. C., Barber, M. J., & Solomonson, L. P. (1993). Expression and characterization of the heme-binding domain of *Chlorella* nitrate reductase. *Journal of Biological Chemistry, 268*, 3268–3271.
26. He, S., Guo, Z., Zhang, Y., Zhang, S., Wang, J., & Gu, N. (2007). Biosynthesis of gold nanoparticles using the bacteria *Rhodopseudomonas capsulate. Materials Letters, 61*, 3984–3987.
27. Gade, A. K., Bonde, P., Ingle, A. P., Marcato, P. D., Durán, N., & Rai, M. K. (2008). Exploitation of *Aspergillus niger* for synthesis of silver nanoparticles. *Journal of Biobased Materials and Bioenerg, 2*, 123–129.
28. Ingle, A., Gade, A., Pierrat, S., Sonnichsen, C., & Rai, M. K. (2008). Mycosynthesis of silver nanoparticles using the fungus *Fusarium acuminatum* and its activity against some human pathogenic bacteria. *Current Nanoscience, 4*, 141–144.
29. Karbasian, M., Atyabi, S. M., Siadat, S. D., Momen, S. B., & Norouzian, D. (2008). Optimizing nanosilver formation by *Fusarium oxysporum* PTCC 5115 employing response surface methodology. *American Journal of Agricultural and Biological Sciences, 3*, 433–437.

30. Thaivanich, S., & Incharoensakdi, A. (2007). Purification and characterization of nitrate reductase from the halotolerant cyanobacterium *Aphanothece halophytica. World Journal of Microbiology and Biotechnology, 23*, 58–92.
31. Laemmli, U. K. (1970). Cleavage of structural proteins during assembly of the head of bacteriophage T4. *Nature, 277*, 680–685.
32. Clark, D. S. (1994). Can immobilization be exploited to modify enzyme activity? *Trends Biotechnology, 12*, 439–443.
33. Huang, J., Lin, L., Li, Q., Sun, D., Wang, Y., Lu, Y., et al. (2008). Continuous-flow biosynthesis of silver nanoparticles by lixivium of sundried *Cinnamomum camphora* leaf in tubular microreactors. *Industrial and Engineering Chemistry Research, 47*, 6081–6090.
34. Clegg, S., Yu, F., Griffiths, L., & Cole, J. A. (2002). The roles of the polytopic membrane proteins NarK, NarU and NirC in *Escherichia coli* K-12: two nitrate and three nitrite transporters. *Journal of Molecular Microbiology, 44*, 143–155.